공학석사 학위논문

편마비 재활을 위한 거울상 로봇 치료 시스템의 개발

Design and Control of a Robotic Mirror Therapy System for Hemiplegia Rehabilitation

2016 년 8 월

서울대학교 대학원

협동과정 바이오엔지니어링 전공

고 석 규

Abstract

Design and Control of a Robotic Mirror Therapy System for Hemiplegia Rehabilitation

By

Sukgyu Koh

Interdisciplinary Program for Bioengineering

The Graduate School

Seoul National University

The objective of study is to design and control a robotic mirror therapy system for hemiplegia rehabilitation. The system induces rehabilitation of an arm functionality by increasing neuroplasticity via combination of a conventional mirror therapy and the robot. Consequently, the robot rehabilitates patients to accomplish the Activities of Daily Living (ADL) tasks.

In order to design hardware of the robotic mirror therapy system, motors were selected first based on calculation using anthropometric data. Entire system was designed to be compact as well as assemblable. Size of the system can be adjusted to fit various wheelchairs and symmetrical structure allows faster transition for either side of the hemiplegic arm. The system uses feedback control based on the motors' information and signals from the AHRS sensors. In order to achieve feedback control, quaternion transformation, kinematics, and inverse kinematics are solved.

The exoskeleton type robotic mirror therapy system has been evaluated its function with an optical motion tracker and confirmed its synchronicity and reaction time. Additionally, the exoskeleton robot was safely tested its function to the normal people as well as to the stroke patients suffering with hemiplegia.

The robotic mirror therapy system can be safely deployed for the sake of rehabilitation for hemiplegic patients. The robot system can also be modified as an exercise robot to increase the hemiparetic arm strength by controlling the impedance. This robotic mirror therapy technology can further develop and apply not only to the upper limbs, but also to lower limbs. In addition to the mirror therapy, other rehabilitation therapy such as unilateral therapies or therapies with virtual reality system may utilize the suggested exoskeleton robot system. Moreover, it can also be adjusted as an assistive device for the hemiparetic patients to assist their ADL tasks. Consequently, the suggested

robotic mirror therapy system could contribute to advancements in the medical field or applied to industrial as well as military applications.

Keywords: Rehabilitation robot, Mirror therapy, Exoskeleton
***Student Number*: 2014-22668**

List of Tables

List of Figures

Table of Contents

1. Introduction

1.1. Background

Population ageing is one of the biggest issue we are facing recently as the birth rate is decreasing and the human lifespan is keep growing over the years through advances in medical care. Among those growing elderly people throughout the world, stroke is one of the most upsurging and deadly disease that they encounter in their ensuing elderhood [1-5]. Stroke accompanies many manifestations such as weakness of the face, limb, vision, or difficulty in speaking [6-8]. Hemiparesis and hemiplegia are both common syndromes due to the stroke: hemiparesis is a condition with weakness of left or right side of the body, while hemiplegia is a condition when one side of the body is fully paralyzed [6,9].

Along with Functional Electrical Stimulation (FES) treatment, mirror therapy is one of the well-known traditional rehabilitation therapy that has successful results in previous studies for the hemiparetic and hemiplegic patients [10,11]. Mirror therapy was initially invented by Ramachandran and employed by Rogers-Ramachandran in 1996 for the limb-amputated patients to allay the manifestation called Phantom limb pain, in which patients feel as if they still have pain in their amputated limb. This traditional mirror therapy utilizes a mirror box to delude the amputees' brain by generating an illusion of having two original limbs

via reflection of the healthy limb as shown in Figure 1.1. By watching the movement of the mirrored limb, which now they conceive it as a normal limb, amputees are deceived as if they are escaping from the pain as they move their phantom limb out of the painful positions [12,13]. Studies showed that the mirror therapy increased motor and sensory cortex excitability, which is associated with neuroplasticity and enhance neuro-rehabilitation [14-21].

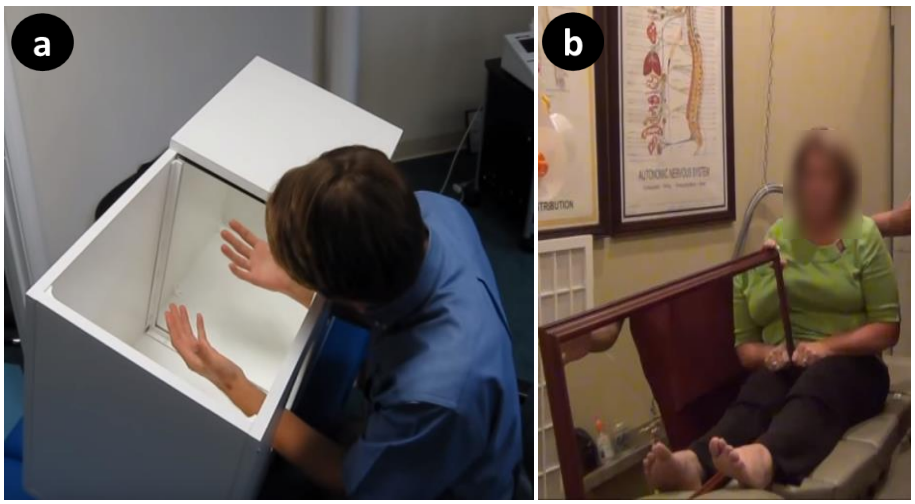

Figure 1.1 (a) Traditional mirror box for upper limb rehabilitation. (b) Mirror therapy for lower limb.

1.2. Research Trends

These days, robot-assisted therapy is rising and promising intervention for the rehabilitation as technology allows us to build and apply it. Robot-assisted rehabilitation therapy is beneficial over the conventional rehabilitation therapy for several reasons. Robotic therapy allows consistent therapies over all patients while conventional human-performed therapy differs every time when therapist performs it, which results unequal outcomes to each patient. In addition, therapists can perform more intense and efficient treatment since the robotic therapy reduces the labor required for the therapists [22,23]. Moreover, the robotic therapy is considered to have benefits by providing the therapists quantitative information about the limb movement such as joint angle range, speed, direction, and torque with high measurement consistency. Furthermore, controlled perturbations into rehabilitation therapy may introduced by the robotic therapy [23,24].

Some of the rehabilitation robots are already deployed in the hospitals with successive outcomes. InMotion ARM, a clinical version of the MIT-MANUS, is an end-effector type robot, which is one of the most practical upper extremity rehabilitation robot clinically proven to improve Functional Independence Measurement (FIM) score [25,26]. Hocoma's ArmeoPower, an exoskeleton type robot based on ARMin technology developed by ETH Zurich, is also a well-known upper limb rehabilitation robotic device that has shown the advantage of the robot-assisted therapy [27]. As for the lower limb

rehabilitation, LokomatPro is one of the most famous gait rehabilitation device that utilizes treadmill to improve its efficiency that showed positive results in clinical studies and improvements in functionalities [28,29]. ReWalk is also a promising lower extremity rehabilitation device in wearable exoskeleton form, which is the only FDA cleared exoskeleton robot for rehabilitation and personal use in the United States [30].

There were several studies for the mirror therapy utilizing the mechanical or electromechanical device as well. The Rocker is a mechanical device for Active-Passive Bimanual movement Therapy (APBT) for wrists. Crankshafts underneath the device allow mirror movement of flexion and extension on the wrists. The study showed inducing cortical excitability before physiotherapy accelerates the recovery of upper extremity function [31]. The Mirror Image Motion Enabler (MIME) is a robotic rehabilitation device that employs the concept of the mirror therapy. A forearm supporting end-effector that mirrors the movement of the healthy arm achieves the motion of the paretic arm [32]. Bi-Manu-Track is a commercially available bilateral robotic arm trainer that provides mirror or symmetric motion. Bi-Manu-Track enables passive or active movement in forearm (pronation- supination) and wrist (flexion-extension) via end-effector handle [33].

Most of commercially available upper limb rehabilitation robots that utilize mirror therapy are in end-effector form; however, end-effector type robot has some drawbacks. First, it only maneuvers the terminal point or link toward the target position where all the other joints and links are following

passively which results the lack of control in transitional motions. This limitation not only induces less accurate quantitative data for the arm positions, but also induces potential injury caused by non-physiological motion.

The exoskeleton type robot has drawbacks of complexity in design and algorithm. Nonetheless, it is worth building the rehabilitation robot in exoskeleton form since it provides full control in each joint. This provides safer operation as well as accurate quantitative information of each joints in motion. The strengths and limitations for end-effector type robots and exoskeleton type robots are presented in Table 1.1 [22].

Figure 1.2 Commercially available rehabilitation robots. (a) InMotion ARM by Interactive Motion Technologies. (b) Armeo Power by Hocoma. (c) LokomatPro by Hocoma. (d) ReWalk by ReWalk Robotics.

Table 1.1 Strengths and limitations for end-effector type robots and exoskeleton type robots [22]

	Strengths	Limitations
End-effector type robots	- Easy setup for each patient - Easy to build, program, and employ it - Manufactured with cheaper expanse	- Only the position of terminal point or link is controlled - Possibility of potential injury from non-physiological motion - Less accurate quantitative data for transitional motion
Exoskeleton type robots	- Full control in each joint configuration - Safer operation - Accurate quantitative data for all individual joints	- A bit more time consuming to setup - Hard to construct and program - Expensive to build

1.3. Objective of Study

The objective of study is to design and control the robotic mirror therapy system for hemiplegia rehabilitation. The system induces rehabilitation of the arm functionality by increasing neuroplasticity via combination of a conventional mirror therapy and the robot, as a result, rehabilitates patients to accomplish the Activities of Daily Living (ADL) tasks. Attitude and Heading Reference System (AHRS) sensors are utilized to achieve the objective of study. To maximize the therapeutic effect, just as conventional mirror therapy, actual mirror is attached in the middle of the system.

2. Materials and Methods

2.1. Hardware Development

Motor Selection

Motors used in the proposed robot system were carefully selected with appropriate torque calculations based on physiological statistic data as specified in Table 2.1 [34]. The posture used for the anthropometric data is depicted as shown in Figure 2.1. Maximum upper limb length for all ages, largest average pushing force, and safety factor of 1.5 were taken into account for sufficient torque production to overcome the patients' paralyzed arm for flawless operation. Weight and center of the gravity for each limb segment are disregarded for the motor selection since the robot is acting only in the yaw direction; the direction of the active torque is acting only on horizontal plane.

As a result, brushless DC motors (EC90flat & EC45flat, Maxon Motor AG, Sachseln, Switzerland) were chosen for safe and robust operation. A motor with maximum 20N·m torque output was selected for the wrist joint and a motor with maximum 50N·m torque output was chosen for the elbow joint. The motors were equipped with hall sensor and encoder for precise position, velocity, and acceleration information.

Table 2.1 Anthropometric data of forearm length and elbow-fist length for Koreans [34]

Length	Average	Standard Deviation	Min.	Max.
Forearm length (mm)	259.3	18.6	205.0	320.0
Elbow-fist length (mm)	314.6	21.0	243.0	413.0
Right arm flexion force (N)	85.6	32.9	34.2	191.4
Left arm extension force (N)	63.5	22.9	22.8	140
Right arm extension force (N)	64.2	22.8	26.7	132.7
Left arm flexion force (N)	83.8	31.9	37.0	180.2

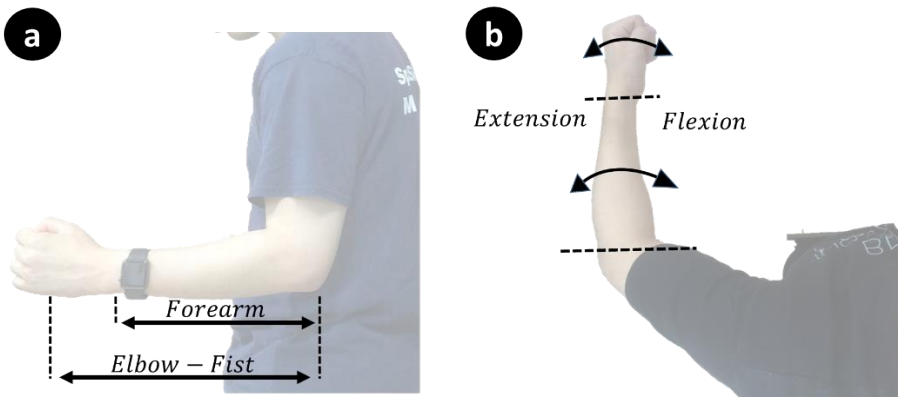

Figure 2.1 (a) Forearm and elbow to fist lengths are defined as shown. (b) Flexion is defined as a rotation toward the body and extension is defined as a rotation away from the body.

Mechanical Design

The entire structure of the exoskeleton robot was designed considering compatibility for the chosen motors and maximum portability. The design was built using 3D CAD software (SOLIDWORKS, SolidWorks Corp., MA, USA).

The robot's frame length can be adjusted according to various human forearm length using shaft and shaft collars. Selected length of the shaft was based on the arm length in Korean anthropometric database [34]. The structure of the robot system including the table is symmetrical. This enables quick and easy transition for either side of the hemiplegic arm; simply placing the robot part of the system into the other side of a pillar on the table and pressing a button on the UI will change the operation side. Frames of a therapy task table can be adjusted such that most of the commercially available wheelchairs can fit into the robot system as shown in Figure 2.2.

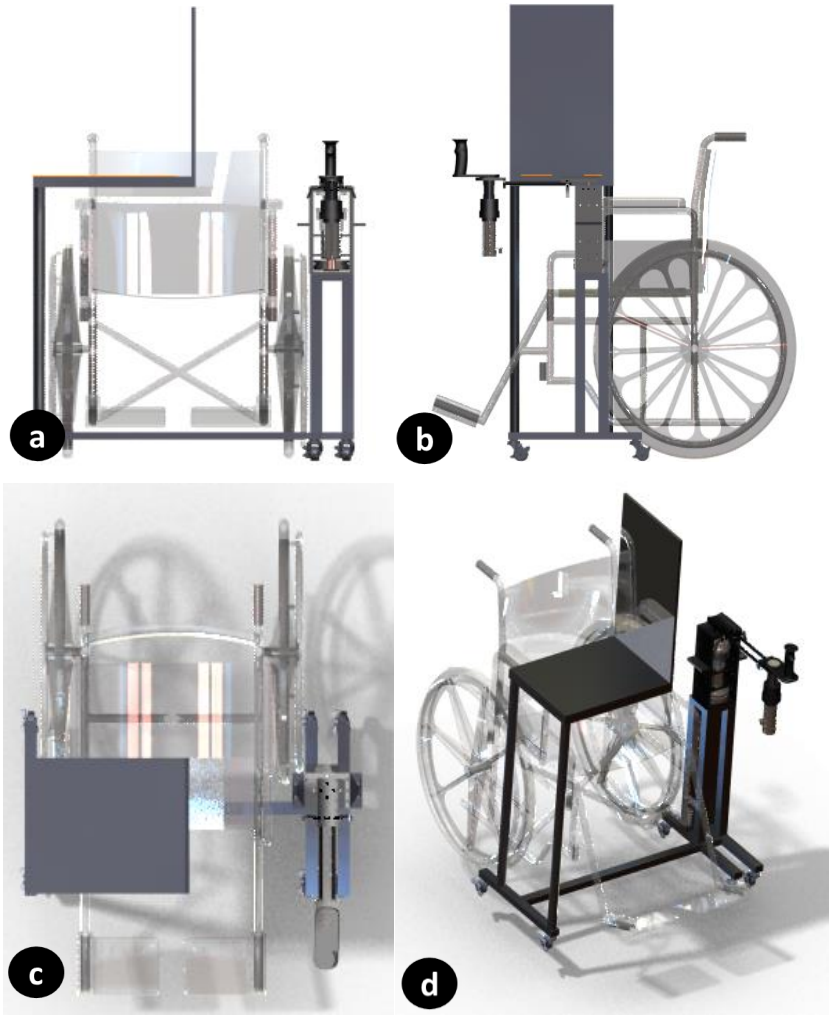

Figure 2.2 Various views of the 3D modeled robotic mirror therapy system with a wheelchair. (a) Front view. (b) Side view. (c) Top view. (d) Dimetric projection of the system.

Two hollow flange reaction torque sensors shown in Figure 2.3-(a) were used to directly detect the reaction torques between the motor and the frame for more precise control and data. These torque sensors were selected according to the maximum torque output of the motors: 20 N·m torque sensor (FT01-20NM, Forsentek, Shenzhen, China) and 50 N·m torque sensor (TFF-500kgf-cm, CTAplus, Daegu, South Korea). As shown in Figure 2.3-(b) and (c), extension shafts for the actuator were manufactured to pass generated torque from the actuator through the flange torque sensor to the body frame. Couplings were used to correct any misalignment between motor shafts and the extension shafts.

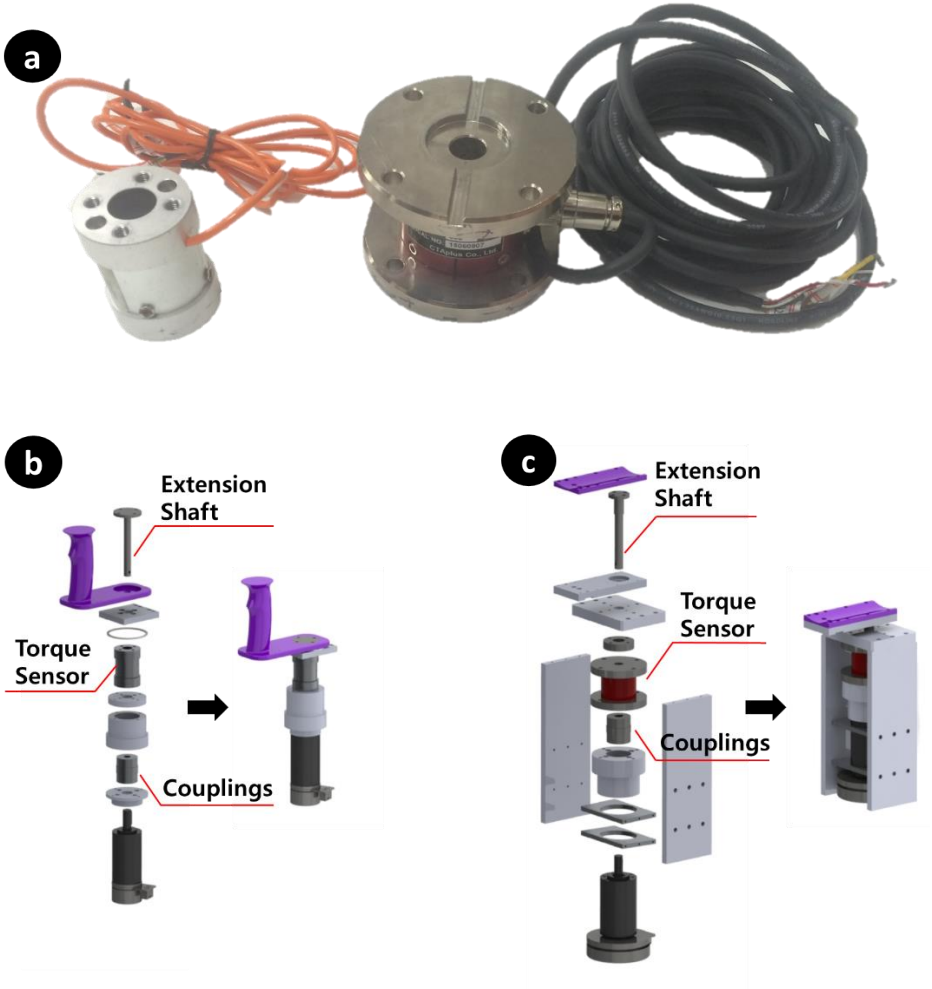

Figure 2.3 (a)Hollow flange torque sensors used for improving the performance of the system. Exploded view and assembled view for (b) wrist and (c) elbow portion.

In addition, wrist joint movement limiter shown in Figure 2.4 was designed and applied to the robot. The purpose of the joint limiter is to prevent misalignment between the robot and the human arm due to severe spasticity as described in Figure 2.5. The joint limiter is designed simple but effective. The limiter is covered with sponges for safety reason and it can adjust its diameter for various patients by adjusting shaft collars. Shaft collar was chosen not only to adjust and fix the part, but also to prevent muscle and tendon injuries when wrist joint stiffness is too high; when the wrist is too firm to fold, the shaft collar will rotate around the shaft and will not forcefully fold the wrist. Therefore, it is crucial not to fasten the collars too tightly when operating with severe spastic patients.

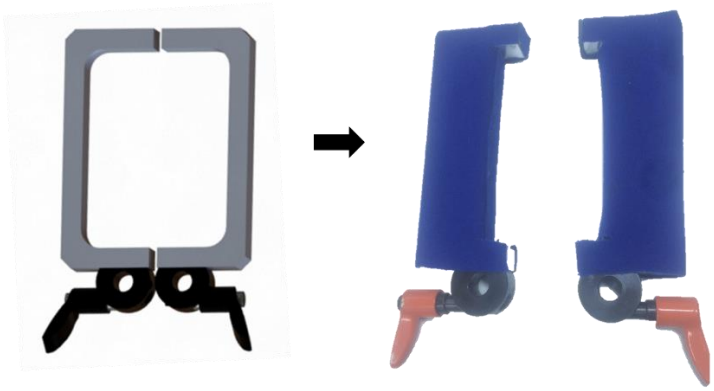

Figure 2.4 (a) Simple CAD design of the wrist joint movement limiter and (b) actual part with sponges wrapped with cloth.

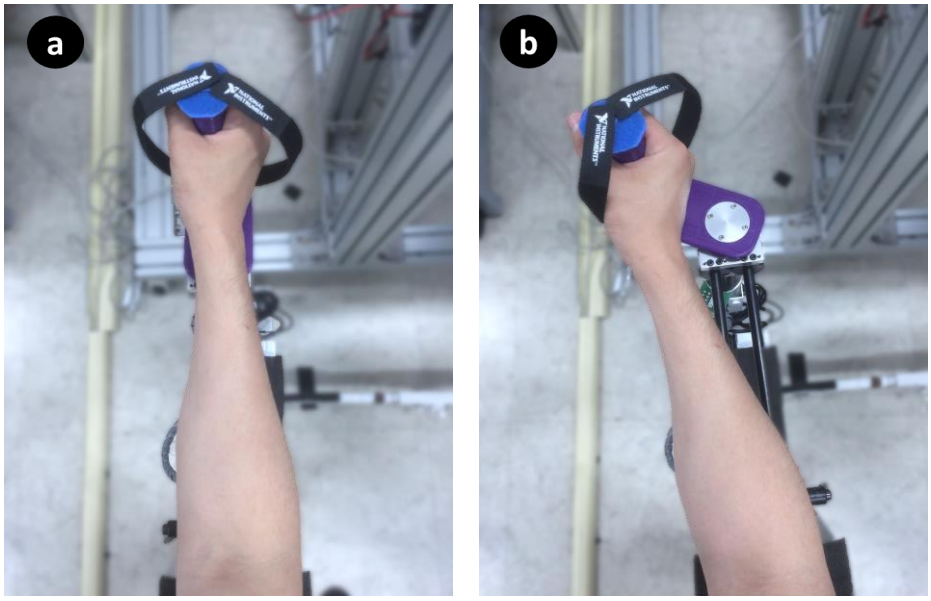

Figure 2.5 (a) Normal position. (b) Misalignment in the robot and the human arm.

Moreover, additional semi-elastic strap, which was chosen with the same reason for the shaft collars, is used to fasten the robot and forearm while preventing muscle and tendon injuries for the patients with high degree of spasticity in elbow.

Every parts that are used in rehabilitation robot were designed to be straightforward and compact while making sure all the parts are assemblable. Also, the parts were designed as simple as possible for easier and faster manufacturing process. CAD design of the entire system is illustrated in Figure 2.6.

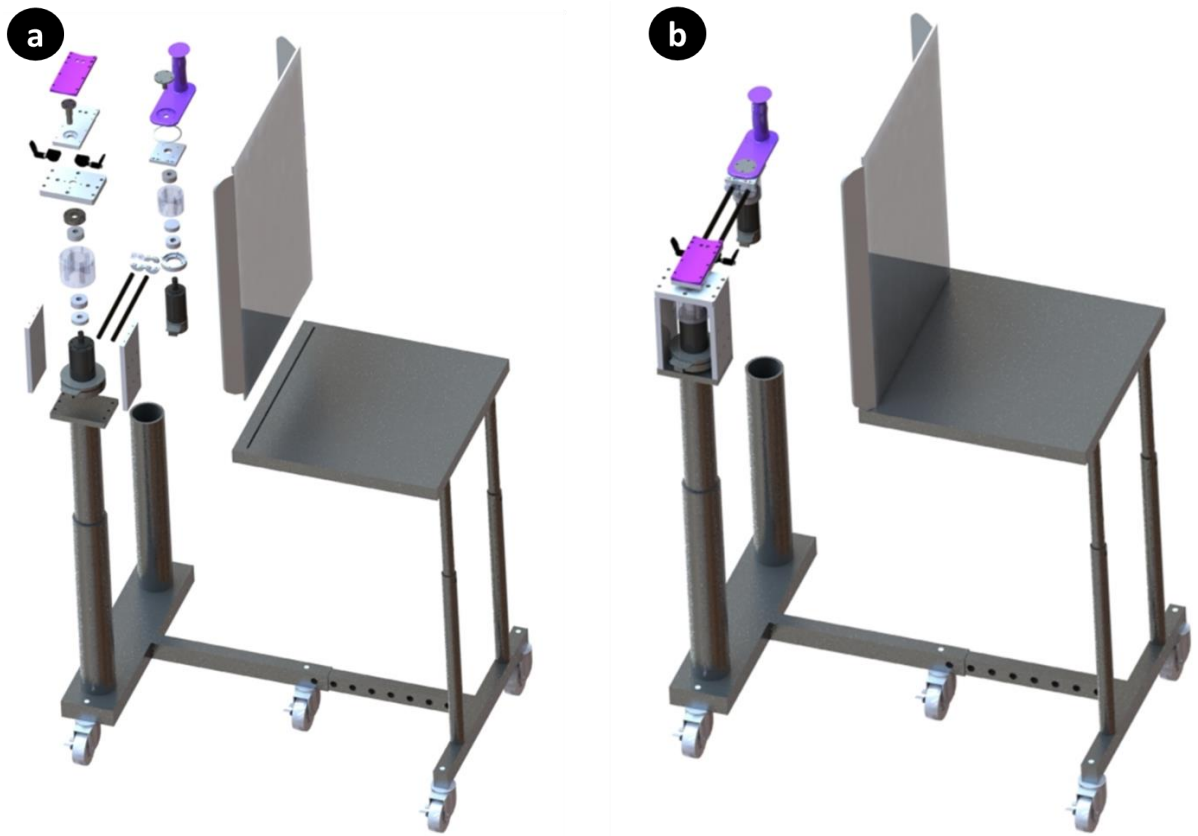

Figure 2.6 (a) Exploded view of all parts in the robot system. (b) Assembled view of the entire robot system.

Attitude and Heading Reference System (AHRS) Sensor

AHRS sensor is a sensor used for modern navigation systems in aircrafts. It is different from the inertial measurement unit (IMU) since it has additional on-board signal processing system to calculate accumulated signals and provide understandable attitude and heading data without any external device. The AHRS sensor consists of accelerometers, gyroscopes, and magnetometers on all x, y, and z-axis; these microelectromechanical instruments provide the attitude as in roll, pitch, and yaw values.

Three wireless AHRS sensors (EBIMU24GV2 ,E2BOX, Seoul, South Korea) and single signal receiver (EBRF24GRCV ,E2BOX, Seoul, South Korea) are used for the mirror therapy exoskeleton system as shown in Figure 2.7-(a). The AHRS sensors are chosen for capturing the motion of the healthy arm since it is not only light-weighted, but also emulous in economic aspect.

Only yaw values are used to represent the arm's attitude since the robot is a 2- Degrees Of Freedom (DOF) planar robot; the DOF (i.e., the rotational movement) of the sensors were restricted by 3D printed supplementary handle and wrist frame to fix the roll and pitch values as shown in Figure 2.7-(b). These sensors are attached to hand and wrist on healthy arm and placed on arbitrary fixed point as a reference coordinate frame as depicted in Figure 2.7-(c) to transfer healthy arm's attitude for controlling the robot.

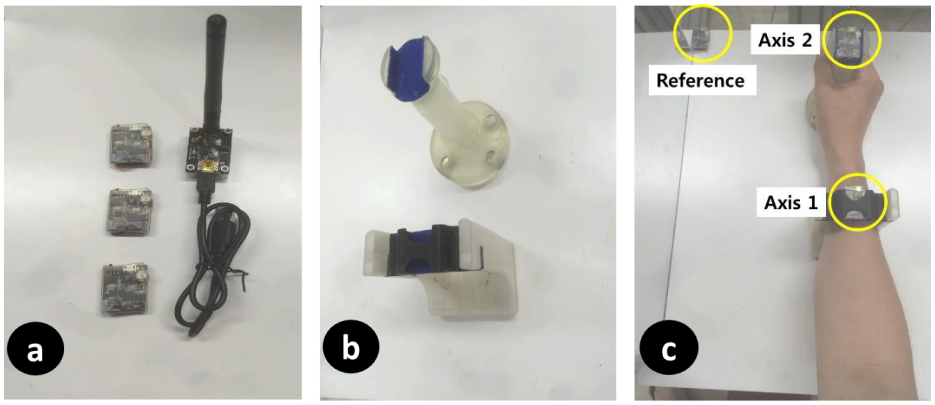

Figure 2.7 (a) Three AHRS sensors and a receiver was used for the system. (b) 3D printed DOF restrictor frame to limit roll and pitch orientations of the sensors to maintain their yaw values. (c) Sensors are set on 3D printed handle, wrist frame, and arbitrary fixed point on a table.

2.2. Development of Control Algorithm

Kinematics

The kinematics of the designed robot system is quite simple since it is a 2-DOF planar robot system (i.e., a two-link manipulator with two rotational joints) as shown in Figure 2.8. Denavit Hartenberg (D-H) convention is used to compute direct kinematics equation for open-loop manipulator by attaching reference coordinate frames. D-H parameters for the proposed robot system are defined in Table 2.2.

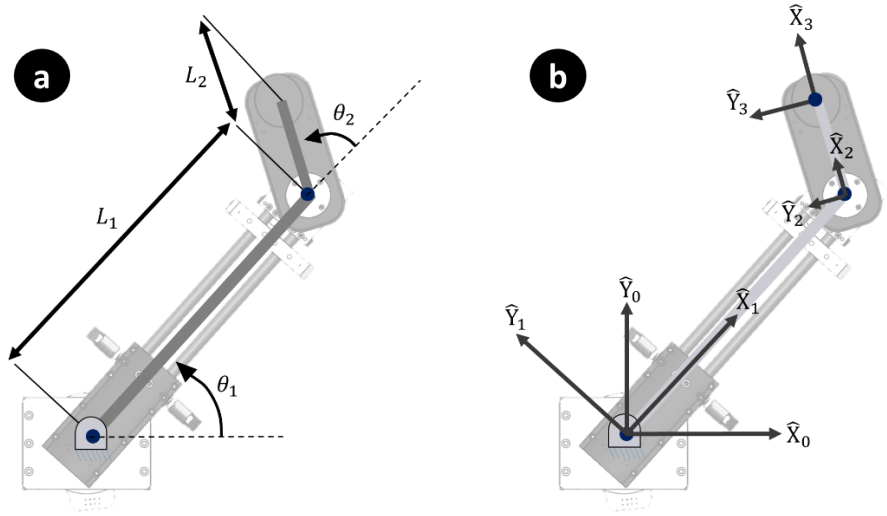

Figure 2.8 (a) Simple 2-DOF planar robot schematics. (b) Coordinate frame assignment for the robot joints.

Table 2.2 D-H parameters for the robot

Link	Link length, a_{i-1}	Link twist, α_{i-1}	Link offset, d_i	Joint angle, θ_i
1	0	0	0	θ_1
2	L_1	0	0	θ_2
3	L_2	0	0	0

The general transformation matrix ${}^{i-1}_{i}T$ is defined as,

$$
\begin{aligned}
{}^{i-1}_{i}T &= \mathrm{Rot}_x(\alpha_{i-1})Trans_x(a_{i-1})Rot_z(\theta_i)Trans_Z(d_i) \\
&= \begin{bmatrix} \cos(\theta_i) & -\sin(\theta_i) & 0 & a_{i-1} \\ \sin(\theta_i)\cos(\alpha_{i-1}) & \cos(\theta_i)\cos(\alpha_{i-1}) & -\sin(\alpha_{i-1}) & -\sin(\alpha_{i-1})\, d_i \\ \sin(\theta_i)\sin(\alpha_{i-1}) & \cos(\theta_i)\sin(\alpha_{i-1}) & \cos(\alpha_{i-1}) & \cos(\alpha_{i-1})\, d_i \\ 0 & 0 & 0 & 1 \end{bmatrix}, \qquad (1)
\end{aligned}
$$

where Rot is the abbreviation for the rotation and Trans is the abbreviation for the Transition [35]. Plugging the values in Table 2.2 into equation (1) result transformation matrixes for the 2-DOF planar robot as shown below:

$$
{}^{0}_{1}T = \begin{bmatrix} c_1 & -s_1 & 0 & 0 \\ s_1 & c_1 & 0 & 0 \\ 0 & 0 & 1 & 0 \\ 0 & 0 & 0 & 1 \end{bmatrix},
$$

$$
{}^{1}_{2}T = \begin{bmatrix} c_2 & -s_2 & 0 & L_1 \\ s_2 & c_2 & 0 & 0 \\ 0 & 0 & 1 & 0 \\ 0 & 0 & 0 & 1 \end{bmatrix},
$$

$$ {}^{2}_{3}T = \begin{bmatrix} 1 & 0 & 0 & L_2 \\ 0 & 1 & 0 & 0 \\ 0 & 0 & 1 & 0 \\ 0 & 0 & 0 & 1 \end{bmatrix}, $$

where $\sin(\theta_i)$ and $\cos(\theta_i)$ are abbreviated as s_i and c_i, respectively.

The end-effector's position due to changes in joint angle can be calculated and represented as a transformation matrix. The transformation matrix from base frame to end-effector frame can be solved by multiplying all transformation matrixes, which is shown below:

$$ {}^{0}_{3}T = {}^{0}_{1}T\,{}^{1}_{2}T\,{}^{2}_{3}T = \begin{bmatrix} r_{11} & r_{12} & r_{13} & p_x \\ r_{21} & r_{22} & r_{23} & p_y \\ r_{31} & r_{32} & r_{33} & p_z \\ 0 & 0 & 0 & 1 \end{bmatrix} $$

$$ = \begin{bmatrix} c_{12} & -s_{12} & 0 & L_2c_{12} + L_1c_1 \\ s_{12} & c_{12} & 0 & L_2s_{12} + L_1s_1 \\ 0 & 0 & 1 & 0 \\ 0 & 0 & 0 & 1 \end{bmatrix} \quad (2) $$

where r represents the rotational elements, p represents position elements, and $\theta_1 + \theta_2$ are abbreviated as subscript 12. From equation (2), velocity matrix at the end-effector can be found by differentiating the position elements.

Jacobian is used to relate joint velocity to end-effector velocity and, as a result, to find the singularities of the system. Singularities indicate there are some configurations that the end-effector cannot move regardless of joint velocities. The Jacobian at the end-effector frame is,

$$ {}^{3}J(\Theta) = \begin{bmatrix} L_1s_2 & 0 \\ L_1c_2 + L_2 & L_2 \end{bmatrix}, \quad (3) $$

and the singularities of the system can be found by letting the determinant of the Jacobian to zero as shown below,

$$\mathrm{Det}\big(J(\Theta)\big) = \mathrm{Det}\begin{bmatrix} L_1 s_2 & 0 \\ L_1 c_2 + L_2 & L_2 \end{bmatrix} = L_1 L_2 s_2 = 0. \qquad (4)$$

Consequently, the singularities are found when the second joint angle θ_2 is at $0°$ and $180°$.

Inverse Kinematics

Desired joint angles for the robot with known link length and end-effector goal position can be calculated using inverse kinematics. From equation (2), position in x axis and position in y axis are expressed as,

$$p_x = L_2 c_{12} + L_1 c_1 \,, \tag{5}$$

$$p_y = L_2 s_{12} + L_1 s_1 \,. \tag{6}$$

Squaring (5) and (6) and summing them will result as,

$$p_x^2 + p_y^2 = L_1^2 + L_2^2 + 2L_1 L_2 c_2. \tag{7}$$

Using (7) and the trigonometric identity, cosine and sine of θ_2 can be calculated and the θ_2 can be calculated using atan2 function as shown below:

$$\theta_2 = atan2(-s_2, \mathrm{c}_2)$$

$$= atan2\left(\pm\sqrt{1 - \left(\frac{p_x^2+p_y^2-L_1^2-L_2^2}{2L_1L_2}\right)^2}, \frac{p_x^2+p_y^2-L_1^2-L_2^2}{2L_1L_2} \right).$$

In order to get θ_1, more complex algebra is applied. Multiplying each side of (5) with $\cos(\theta_1)$ and multiplying each side of (6) with $\sin(\theta_1)$, and summing these two will result as,

$$-c_1 p_x + s_1 p_y = L_1 + L_2 c_2 \tag{8}$$

Also, multiplying each side of (5) with -sin(θ_1) and multiplying each side of (6) with cos(θ_1), and summing these two will result as,

$$-s_1 p_x + c_1 p_y = L_2 s_2 \tag{9}$$

Multiplying (8) with p_x and multiplying (9) with p_y and adding two equations will result as,

$$c_1\left(p_x^2 + p_y^2\right) = p_x(L_1 + L_2 c_2) + p_y L_2 s_2 \tag{10}$$

With (10) and the trigonometric identity, cosine and sine of θ_2 can be calculated and the θ_2 can be calculated using atan2 function as shown below:

$$\theta_1 = atan2(s_1, c_1)$$

$$= atan2\left(\pm\sqrt{1 - \left(\frac{p_x(L_1 + L_2 c_2) + p_y L_2 s_2}{p_x^2 + p_y^2}\right)^2}, \frac{p_x(L_1 + L_2 c_2) + p_y L_2 s_2}{p_x^2 + p_y^2}\right)$$

Calculated θ_1 and θ_2 are then referred for a feedback control.

Sensor signal processing

Sensor signal from the AHRS sensor provides either Euler angle format or quaternion format as an output. The proposed system uses quaternion output since it eliminates the concern for the singularities and it reduces the computation time for the software algorithm [36,37].

Quaternion is a set of four parameters: one real value and three imaginary values as shown below:

$$q = \eta + \epsilon_x i + \epsilon_y j + \epsilon_z k\ ,$$

where η is the real value and all the rest are the imaginary values.

The rotation matrix R as in quaternions can be represented as shown below:

$$\mathrm{R} = \begin{bmatrix} \eta^2 + \epsilon_x^2 - \epsilon_y^2 - \epsilon_z^2 & 2(\epsilon_x\epsilon_y - \eta\epsilon_z) & q(\epsilon_x\epsilon_z + \eta\epsilon_y) \\ 2(\epsilon_x\epsilon_y + \eta\epsilon_z) & \eta^2 - \epsilon_x^2 + \epsilon_y^2 - \epsilon_z^2 & 2(\epsilon_y\epsilon_z - \eta\epsilon_x) \\ 2(\epsilon_x\epsilon_z - \eta\epsilon_y) & 2(\epsilon_y\epsilon_z + \eta\epsilon_x) & \eta^2 - \epsilon_x^2 - \epsilon_y^2 + \epsilon_z^2 \end{bmatrix}$$

This rotation matrix is then calculated for the roll, pitch, and yaw angles as shown below:

$$\phi = \begin{cases} atan2\left(2(\epsilon_y\epsilon_z + \eta\epsilon_x), (\eta^2 - \epsilon_x^2 - \epsilon_y^2 + \epsilon_z^2)\right) & -\frac{\pi}{2} < \theta < \frac{\pi}{2} \\ atan2\left(-2(\epsilon_y\epsilon_z + \eta\epsilon_x), -(\eta^2 - \epsilon_x^2 - \epsilon_y^2 + \epsilon_z^2)\right) & \frac{\pi}{2} < \theta < \frac{3\pi}{2} \end{cases}$$

$$\theta = \mathrm{asin}\left(-2(\epsilon_x\epsilon_z - \eta\epsilon_y)\right)$$

$$\psi = \begin{cases} atan2\left(2\left(\epsilon_x\epsilon_y + \eta\epsilon_z\right), \left(\eta^2 + \epsilon_x^2 - \epsilon_y^2 - \epsilon_z^2\right)\right) & -\frac{\pi}{2} < \theta < \frac{\pi}{2} \\ atan2\left(-2\left(\epsilon_x\epsilon_y + \eta\epsilon_z\right), -\left(\eta^2 + \epsilon_x^2 - \epsilon_y^2 - \epsilon_z^2\right)\right) & \frac{\pi}{2} < \theta < \frac{3\pi}{2} \end{cases}$$

Since the robot is a simple 2-DOF planar robot on horizontal plane, only yaw value ψ is used to feed as a desired angle for the actuators.

Control Protocol

The process of the programmed algorithm is quite straightforward as shown in block scheme Figure 2.9. First, when the program is turned on, the robot initializes its position to a pre-defined initial position. Then, it goes into a main loop for actual therapy process with feedback control. Joint angles from AHRS sensors and desired angles from inverse kinematics incorporate each other to achieve the feedback control. Each iteration of the loop, the encoder and hall sensor in each motor checks the actuator status and feed the desired information into the control algorithm while the sensors keep feed the captured angles of the healthy arm's joints in real-time. When the physical therapist terminates the program, it will come back to the pre-defined initial position and finishes the therapy process.

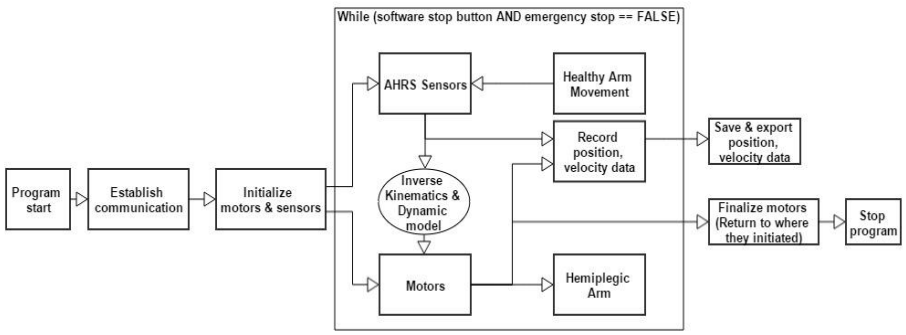

Figure 2.9 A block scheme for the software protocol.

Motor Assessment Scale (MAS) is the one of the ways to scale the patient's spasticity. When assessing the MAS, it is often safer to stop once and move on slowly afterwards if the therapist feel sudden large resistance in a patient's limb. This procedure reduces the chance of permanent impairment in their arm. Just as when the physical therapist assesses the MAS, the robot rapidly stops and then move slowly for further desired trajectory if the reaction torque detected by the torque sensor is over the safety threshold.

Application of the torque sensor also helps the feedback control for the smoother operation. Signal from the torque sensors is cooperated with the AHRS sensors and deliver appropriate velocity to smooth cooperation between human arm, sensors, and actuators. This protocol is implemented as in sequence structure with real-time system design software (LabVIEW 2013, National Instruments, TX, USA) for real-time control operation as depicted in Figure 2.10.

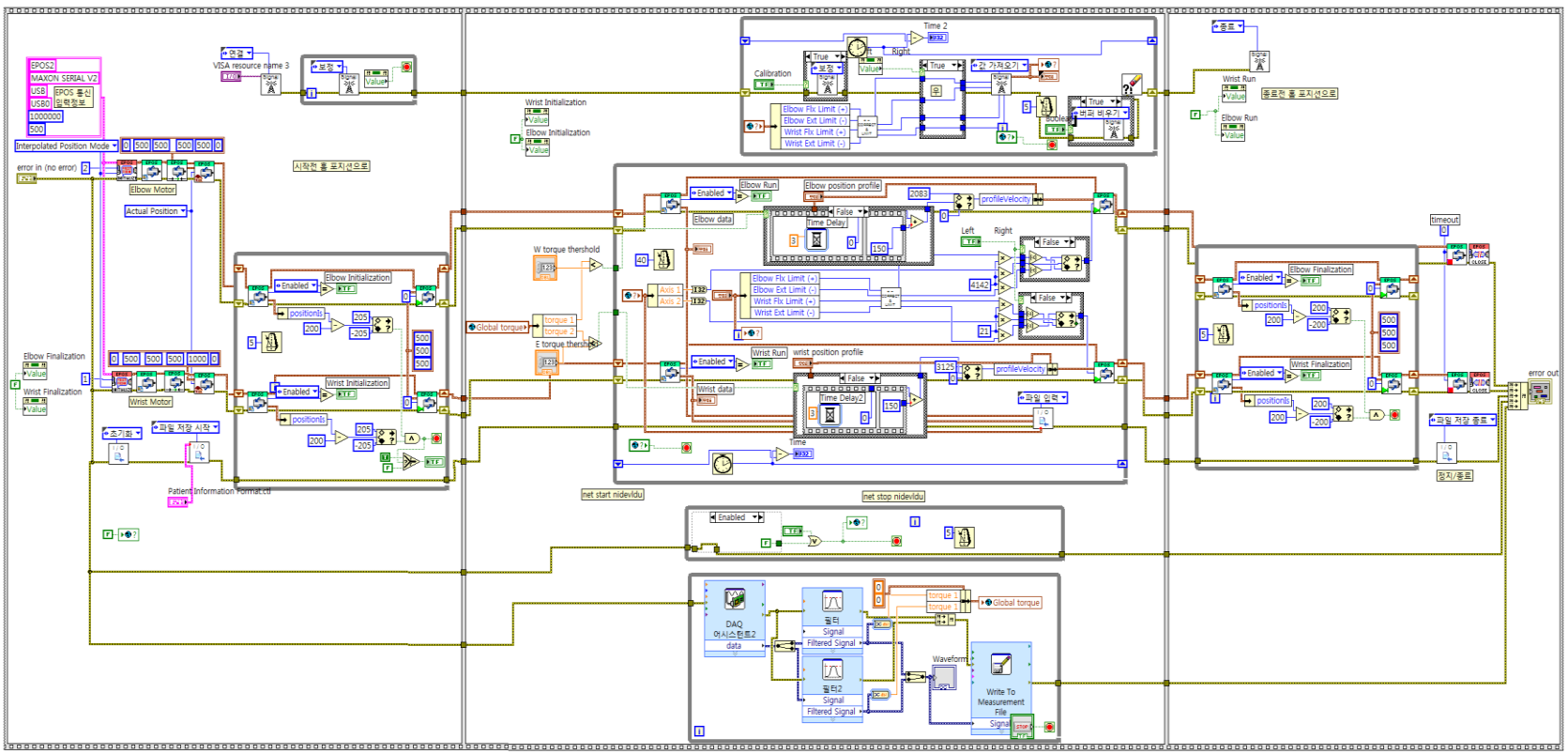

Figure 2.10 Software protocol of the rehabilitation robot system implemented in LabVIEW.

User Interface

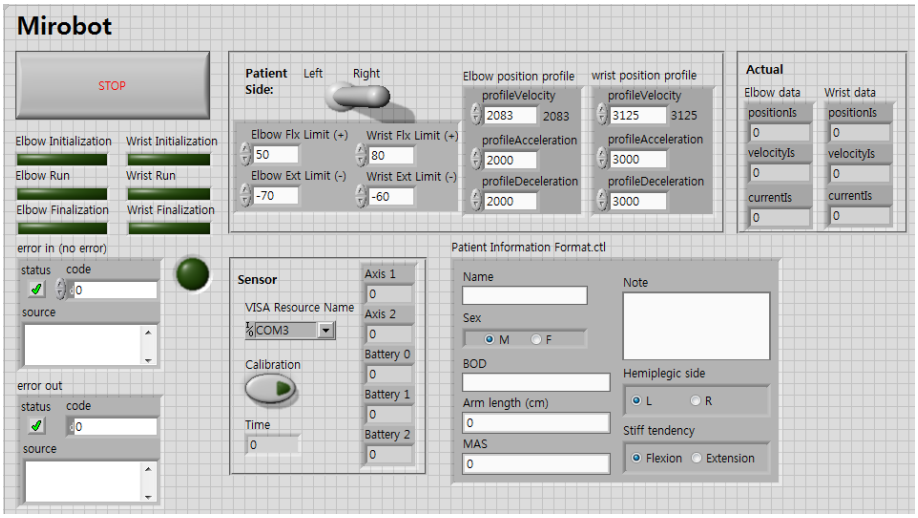

Figure 2.11 User interface of the rehabilitation robot system.

The physical therapist can control and monitor the exoskeleton robot system via User Interface (UI) in the LabVIEW program as shown in Figure 2.11; this UI enables the therapist to acknowledge the quantitative information and adjust appropriate control input to the robot for proper operation.

The UI consists of the LEDs that specify the current run status and error indicators for troubleshooting. Physical therapist can type in information about the patient to discriminate each patient. Also, the therapist can choose operation side (i.e., either left or right side) according to the patient's hemiplegic side by pressing the patient side. In addition, the operation angle limit for each joint can be defined in real-time for safe operation. Inside the program, ranges of angle values are strictly set to $0\sim50°$ for elbow flexion, $0\sim70°$ for elbow extension, $0\sim80°$ for wrist flexion, and $0\sim60°$ for wrist extension for safety

reason. Moreover, the therapist can manually configure the actuator velocity, acceleration, and deceleration in real-time as well. Furthermore, the position, velocity, and acceleration information of the robot are displayed in the “Actual” box while it displays the patient’s arm joint angle and sensor battery remains in “Sensor” box. This enables the therapist to check the status of the robot and sensors in real-time and monitor the overall progress of the therapy.

In order to calibrate the sensor error caused from gyro drift, calibration button is added on the UI to constantly calibrate position error between the sensor readings and actual position.

2.3. Evaluation

Evaluation of the developed robot system was proceeded to confirm its synchronicity and response time. Optical motion tracker system (PST Base, PS-Tech, Amsterdam, Netherlands) was used for capturing motion of the robot.

Optical passive markers with distinctive patterns shown in Figure 2.12-(a) was devised and trained via motion tracking software in order to differentiate objects recognized by the motion tracker. These markers are attached on end-effector, wrist joint, wrist restrictor, and elbow joint of the robot system and corresponding positions on the human arm side as shown in Figure 2.12-(b).

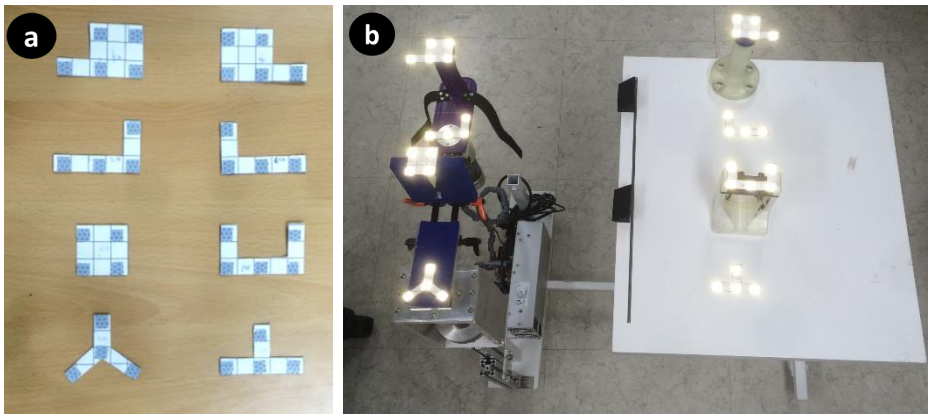

Figure 2.12 (a) Optical markers with distinctive patterns for differentiating the recognized objects by the motion tracker. (b) Position of the markers for the validation process.

The environment for validation process was set as shown in Figure 2.13. The optical motion capture system was held directly on top of the robot system for accurate trajectory analysis.

Position as well as orientation information of the arm and robot was simultaneously collected via motion capturing software as shown in Figure 2.14. Random movement was captured for 5 times about 3 minutes each. These captured data was processed in MATLAB for trajectory and orientation error analysis.

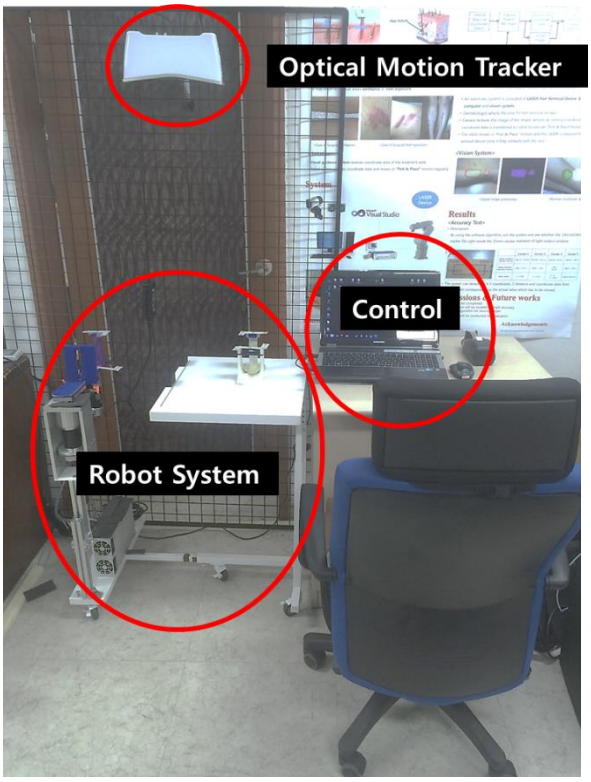

Figure 2.13 The environment for validation process. Optical motion tracker was held directly on top of the robot system for the validation process.

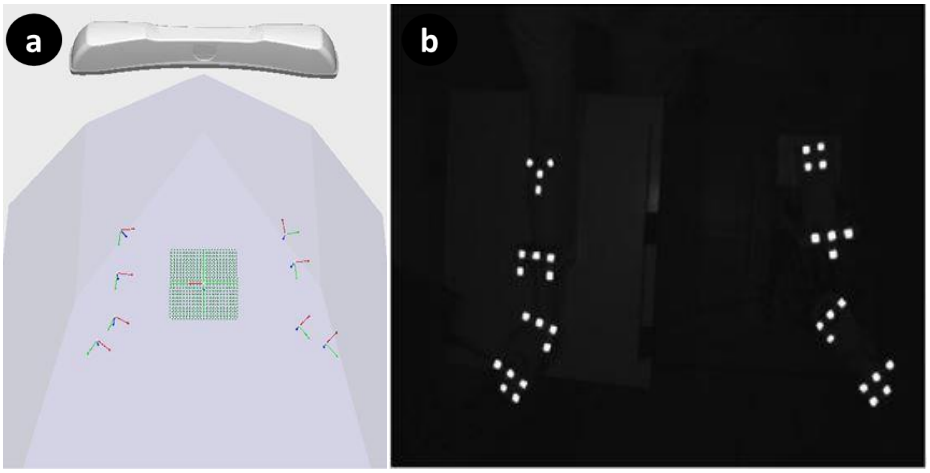

Figure 2.14 The motion tracker software displays the (a) position and orientation of the markers and (b) the actual image getting from the camera.

3. Results

The weight of the robot system is 18kg and the volume can be adjusted from as large as 0.303 m^3 for various types of wheelchairs (from standard manual wheelchairs to electric powered wheelchairs) to as small as 0.145 m^3 for convenient storage. The final product of the robot is shown in Figure 3.1 and detailed information about the final product of the robot is specified in Table 3.1.

Figure 3.1 (a) Final product of the robotic mirror therapy system for hemiplegia rehabilitation. (b) Adjustable size specification.

Table 3.1 Specification of the robotic mirror therapy system

Volume (m^3)	0.145 - 0.303
Size adjustability	O
Maximum torque output on wrist (N·m)	20
Maximum torque output on elbow (N·m)	50
Entire system weight (kg)	18
Symmetric structure	O
Operation side transition time (s)	60 <
Response time (s)	0.04 – 0.4

The captured motion tracking data was processed in MATLAB for trajectory and orientation error analysis as shown in Figure 3.2. Resulted errors between the robot and the human arm are calculated and tabulated in Table 3.2

Table 3.2 Result of the validation using optical motion tracker

	Hand	Wrist	Forearm	Elbow
Number of data	1765			
Mean angle error (°)	4.60	3.53	2.08	1.97
Angle RMSE	4.45	4.89	2.60	2.53
Angle variance	8.57	8.53	2.44	2.50
Overall error (%)	3.28	2.52	1.73	1.64
Mean position error (cm)	0.07	0.16	0.05	0.12
Position RMSE	0.07	0.16	0.05	0.12
Position variance	0.00 (0.00013)	0.00 (0.00067)	0.00 (0.000075)	0.00 (0.00035)

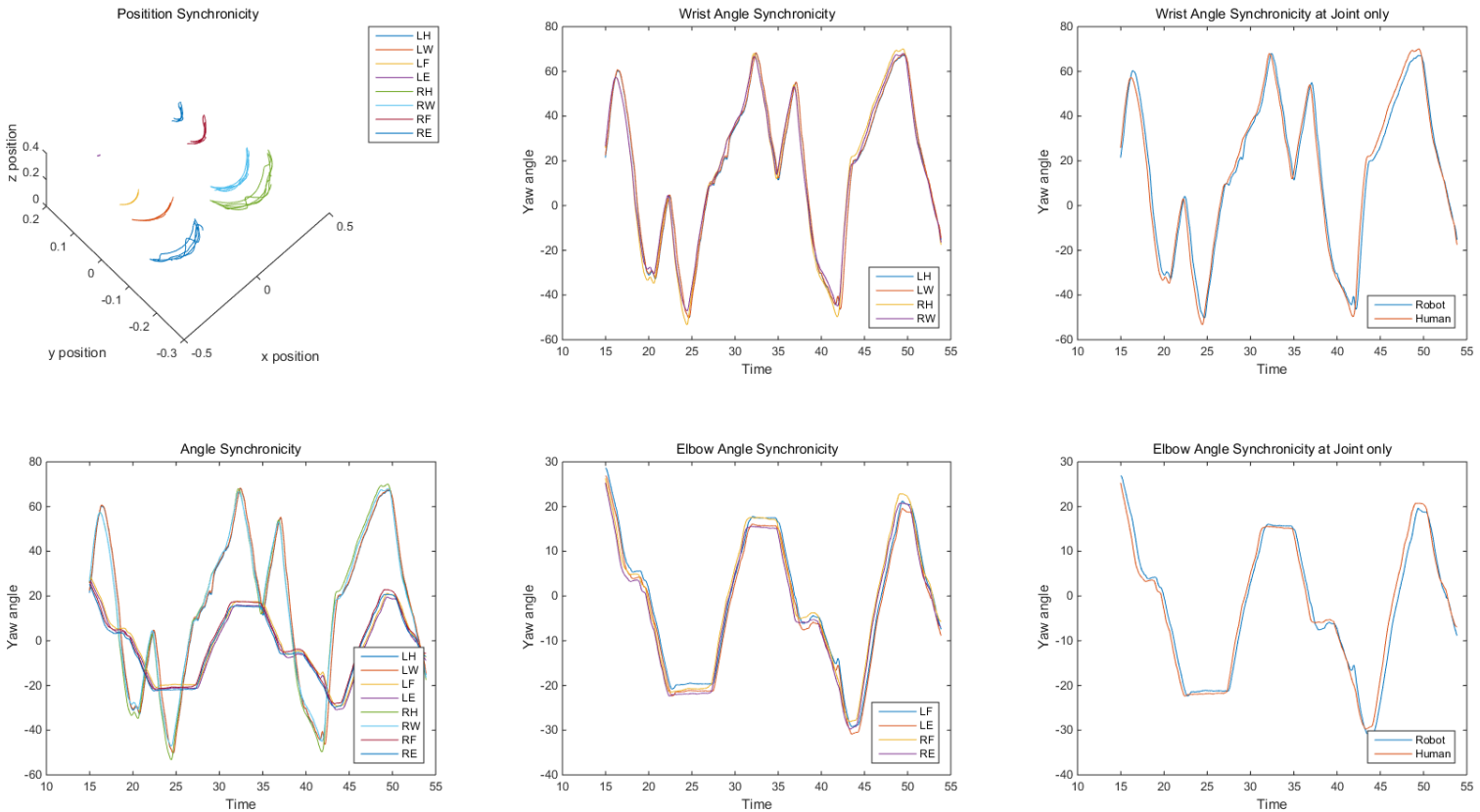

Figure 3.2 Trajectory analysis processed in MATLAB. Abbreviations: LH-Robot hand, LW-Robot wrist, LF-Robot Forearm, LE-Robot elbow, RH-Human hand, RW-Human wrist, RF-Human Forearm, RE-Human elbow.

4. Discussion

The therapist carried the robotic mirror therapy system around the hospital with ease and stored the system without occupying a lot of space. Also, patients with MAS grade less than 3 are tried the clinical trials and the robot system showed flawless operation with enough torque output. Synchronicity is crucial for increasing the induction in neuroplasticity. The developed robotic therapy system showed response time ranging from 0.04 sec to 0.4 sec; human barely recognize this delay time and, therefore, the system proved its synchronicity. Furthermore, mean angle error during the operation showed less than 5 degrees. Maximum percent error for the operation range is 3.28%. Also, the position error is less than 0.2 cm for all position. These results prove the suggested robotic mirror therapy system's functionality.

Current limitation of the developed robotic mirror therapy robot system is that there is too much gyro drift in the AHRS sensors, which mislead the robot from actual trajectory of the arm when the operation takes long time. Consequently, the therapist should constantly calibrate the sensors during the therapy session. This drawback can be solved by making sensors with filter and separating the measurement unit with the accelerometer, or simply get more stable commercially available alternative sensors. In addition, the robot system lacks DOF for the most of the ADL tasks. Although the hemiplegic patients who tried the clinical trials were very satisfied with the robot system during the clinical trial, mirrored arm movement in planar plain is too confined to

rehabilitate arm for the most of the ADL tasks. The system is recommended to be upgraded to achieve general ADL tasks by increasing the DOF.

5. Conclusion

In this study, a robotic mirror therapy system for hemiplegia rehabilitation was designed and controlled. The exoskeleton type robotic mirror therapy system has been evaluated its function with an optical motion tracker and confirmed its synchronicity and reaction time. Additionally, the exoskeleton robot was safely tested its function to the normal people as well as stroke patients suffering with the hemiplegia.

The suggested robot system can be modified as an exercise robot to increase the hemiparetic arm strength by controlling the impedance. This robotic mirror therapy technology can further develop and apply to the lower limbs as well. In addition to the mirror therapy, other rehabilitation such as unilateral therapies or therapies with virtual reality system may utilize the suggested exoskeleton robot system. Moreover, it can also be adjusted as an assistive device for the hemiparetic patients to assist their ADL tasks. Consequently, the suggested robotic mirror therapy system could contribute to advancements in the medical field or be applied to industrial as well as military applications.

References

[1] Arnan, Martinson K., Gregory L. Burke, and Cheryl Bushnell. "Secondary prevention of stroke in the elderly: focus on drug therapy." Drugs & aging 31.10 (2014): 721-730.

[2] Bacigaluppi, Marco, et al. "Influence of age-related blood brain barrier modifications on the outcome of experimental stroke in elderly mice." Journal of Neuroimmunology 275.1 (2014): 27.

[3] Collins, Donna. “Rehabilitation of the Elderly Stroke Patient.” Canadian Family Physician 27 (1981): 1595–1597. Print.

[4] Mozaffarian, Dariush, et al. "Executive Summary: Heart Disease and Stroke Statistics—2016 Update A Report From the American Heart Association." Circulation 133.4 (2016): 447-454.

[5] Nelles, Gereon, et al. "Reorganization of Sensory and Motor Systems in Hemiplegic Stroke Patients A Positron Emission Tomography Study." Stroke 30.8 (1999): 1510-1516.

[6] Fisher, C. Miller, and H. B. Curry. "Pure motor hemiplegia of vascular origin." Archives of neurology 13.1 (1965): 30.

[7] Judd, Suzanne E., et al. "Self-report of stroke, transient ischemic attack, or stroke symptoms and risk of future stroke in the REasons for Geographic and Racial Differences in Stroke (REGARDS) study." Stroke 44.1 (2013): 55-60.

[8] Lisabeth, Lynda D., et al. "Acute Stroke Symptoms Comparing Women and Men." Stroke 40.6 (2009): 2031-2036.

[9] Altschuler, Eric Lewin, et al. "Rehabilitation of hemiparesis after stroke with a mirror." *The Lancet* 353.9169 (1999): 2035-2036.

[10] Handa, Yasunobu. "Yuji Inagaki, Kazunori Seki1, Takahide Ogura2, Takaaki Sekiya3."

[11] Teasell, Robert. "Upper Extremity Interventions."

[12] Ramachandran, Vilayanur S., Diane Rogers-Ramachandran, and Steve Cobb. "Touching the phantom limb." Nature 377.6549 (1995): 489-490.

[13] Ramachandran, Vilayanur S., and Diane Rogers-Ramachandran. "Synaesthesia in phantom limbs induced with mirrors." Proceedings of the Royal Society of London B: Biological Sciences 263.1369 (1996): 377-386.

[14] Brokaw, Elizabeth B., et al. "Robotic therapy provides a stimulus for upper limb motor recovery after stroke that is complementary to and distinct from conventional therapy." *Neurorehabilitation and neural repair* (2013): 1545968313510974.

[15] Diers, Martin, et al. "Mirrored, imagined and executed movements differentially activate sensorimotor cortex in amputees with and without phantom limb pain." PAIN® 149.2 (2010): 296-304.

[16] Ezendam, Daniëlle, Raoul M. Bongers, and Michiel JA Jannink. "Systematic review of the effectiveness of mirror therapy in upper extremity function."*Disability and rehabilitation* 31.26 (2009): 2135-2149.

[17] Luft, Andreas R., et al. "Repetitive bilateral arm training and motor cortex activation in chronic stroke: a randomized controlled trial." Jama 292.15 (2004): 1853-1861.

[18] Oujamaa, L., et al. "Rehabilitation of arm function after stroke. Literature review." Annals of physical and rehabilitation medicine 52.3 (2009): 269-293.

[19] Rizzolatti, Giacomo, Maddalena Fabbri-Destro, and Luigi Cattaneo. "Mirror neurons and their clinical relevance." Nature Clinical Practice Neurology 5.1 (2009): 24-34.

[20] Small, Steven L., Giovanni Buccino, and Ana Solodkin. "The mirror neuron system and treatment of stroke." Developmental psychobiology 54.3 (2012): 293-310.

[21] Thieme, Holm, et al. "Mirror therapy for improving motor function after stroke." Stroke 44.1 (2013): e1-e2.

[22] Poli, Patrizia, et al. "Robotic technologies and rehabilitation: new tools for stroke patients' therapy." BioMed research international 2013 (2013).

[23] Huang, Vincent S., and John W. Krakauer. "Robotic neurorehabilitation: a computational motor learning perspective." Journal of NeuroEngineering and Rehabilitation 6.1 (2009): 5.

[24] Hidler, Joseph, and Robert Sainburg. "Role of robotics in neurorehabilitation." Topics in spinal cord injury rehabilitation 17.1 (2011): 42.

[25] Interactive Motion Technologies. URL: http://interactive-motion.com/healthcarereform/upper-extremity-rehabilitiation/inmotion2-arm/

[26] Aisen, Mindy Lipson, et al. "The effect of robot-assisted therapy and rehabilitative training on motor recovery following stroke." *Archives of neurology* 54.4 (1997): 443.

[27] https://www.hocoma.com/usa/us/products/armeo/armeopower/

[28] https://www.hocoma.com/usa/us/products/lokomat/lokomatpro/

[29] Dundar, U., et al. "A comparative study of conventional physiotherapy versus robotic training combined with physiotherapy in patients with stroke."*Topics in stroke rehabilitation* 21.6 (2014): 453-461.

[30] ReWalk Robotics. URL: http://rewalk.com/

[31] Stinear, James W., and Winston D. Byblow. "Rhythmic bilateral movement training modulates corticomotor excitability and enhances upper limb motricity poststroke: a pilot study." *Journal of Clinical Neurophysiology* 21.2 (2004): 124-131.

[32] Burgar, Charles G., et al. "Development of robots for rehabilitation therapy: the Palo Alto VA/Stanford experience." *Journal of rehabilitation research and development* 37.6 (2000): 663-674.

[33] Hesse, Stefan, et al. "Robot-assisted arm trainer for the passive and active practice of bilateral forearm and wrist movements in hemiparetic subjects."*Archives of physical medicine and rehabilitation* 84.6 (2003): 915-920.

[34] *Size Korea*, Korean Agency for Technology and Standards <http://sizekorea.kats.go.kr/>

[35] Siciliano, Bruno, et al. “Robotics: modelling, planning and control.” Springer Science & Business Media, (2010).

[36] Schwab, Arend L. "Quaternions, finite rotation and euler parameters." *See also URL http://audiophile. tam. cornell. edu/~ als93/Publications/quater nion. pdf* (2002).

[37] W. Kim. "A study on the development of 6-DOF wearable mirror therapy robot system." *master's thesis*. Retrieved from Seoul National University Library data base.

국문초록

편마비 재활을 위한 거울상 로봇 치료 시스템의 개발

고석규

서울대학교 대학원

협동과정 바이오엔지니어링 전공

본 연구는 편마비 환자들이 일상생활활동 동작을 수행할 수 있도록 재활을 돕는 외골격 형태의 거울상 로봇 치료 시스템의 개발을 목적으로 한다. 본 연구에서 개발 된 로봇 시스템은 실제 거울을 이용하는 거울치료를 외골격 로봇과 융합하여 마비된 팔에 직접적인 움직임을 유도함으로서 치료를 증진한다.

본 연구에서 개발된 시스템에서 사용된 모터는 인체측정학의 통계자료를 참조하여 계산된 적정 토크 값을 출력할 수 있는 모터를 선정하였고, 전체 시스템은 간략하면서도 조립가능성을 고려하여 설계 되었다. 로봇 시스템의 사이즈는 여러

휠체어에 맞게 조정이 가능하며, 대칭적인 구조는 팔의 좌우에 관계없이 빠른 전환이 가능하게 설계되었다. 로봇의 제어는 자세방위기준장치 센서의 쿼터니언 출력 값의 변환, 엔코더와 홀센서에서 얻을 수 있는 모터내부 정보를 이용해 기구학 및 역기구학을 이용하여 피드백 제어를 적용하였다.

본 연구에서 개발 된 로봇 시스템은 팔과 로봇의 궤적에서의 동시성과 반응시간을 확인함으로서 평가되었다. 로봇과 팔의 움직임은 광학센서를 이용하여 여러 움직임을 정밀하게 측정하였고 팔의 위치와 방향 정보는 MATLAB을 통한 궤도분석으로 그 성능을 입증하였다.

본 연구에서 개발된 상지 재활 로봇은 편마비 환자의 재활을 위해 효과적이고 안전하게 적용될 수 있다. 또한 저항을 제어함으로서 근력 운동 기기로도 변형이 가능 하며, 나아가 거울상 치료가 아닌 한쪽 팔만 사용하는 치료, 가상현실 기술을 접목한 치료, 일상생활 보조기기에도 활용될 수 있다. 그 뿐만 아니라 산업적이나 군사적 목적으로도 기여할 수 있을 것이다.

주요어: 재활 로봇, 거울상 치료, 외골격 로봇
학 번: 2014-22668